Subband Coding and Noise Reduction in Multiresolution Analysis Frames

John J. Benedetto† and *Shidong Li**
†Department of Mathematics,
University of Maryland, College Park, MD 20742
and
The MITRE Corporation
*Department of Mathematics and Computer Scieneces
6211 Sudikoff Laboratory
Dartmouth College
Hanover, NH 03755

Dedicated to the memory of C. H. Cook

Abstract

We consider the effect of the quantization noise introduced by coding at subbands. We demonstrate that significant noise reduction is achieved by using wavelet frames and their associated filter banks in a subband signal processing system.

1 Introduction

We have recently defined and characterized a frame multiresolution analysis (FMRA) [1], [3], in which subspaces at each resolution are generated by an arbitrary affine frame formed by translates and dilates of a single function ϕ.

Subband coding has its roots in speech and image signal processing. In a complete subband coding system, a given signal is first filtered through a band-limited filter (which provides a least square approximation of the signal in a proper subspace of band-limited functions) and sampled. Then the sampled signal is split into several subbands and coded according to certain prescribed or perceptual criteria. This data is then transmitted. At the receiver side, the data is decoded, combined and interpolated to obtain the original signal.

As in every communication system, the quantization and/or coding, as well as transmission processes in a subband coding system, involve noise interference. As a key element of a subband processing system, the quantization and the noise introduced at subbands are important issues to be studied in any real subband system, e.g., [5], [9], [11], [13]. We study a complete subband signal processing system in *frame multiresolution subspaces* and demonstrate that the redundant nature of the frame representation provides substantial noise reduction.

0-8194-1627-4/94/$6.00

2 Frame Multiresolution Analysis and Subband Processing

To describe what frame multiresolution subspaces are, we shall begin with the definition of frame multiresolution analysis.

Definition 2.1 A *frame multiresolution analysis* (FMRA) of $L^2(\mathbf{R})$ is an increasing sequence of closed linear subspaces $V_j \subseteq L^2(\mathbf{R})$ and an element $\phi \in V_0$ for which the following hold:

(i) $\overline{\cup_j V_j} = L^2(\mathbf{R})$ and $\cap_j V_j = 0$,

(ii) $f(t) \in V_j$ if and only if $f(2t) \in V_{j+1}$,

(iii) $f \in V_0$ implies $\tau_k f \in V_0$, for all $k \in \mathbf{Z}$, where $\tau_k f(t) \equiv f(t-k)$,

(iv) $\{\tau_k \phi : k \in \mathbf{Z}\}$ is a frame for the subspace V_0.

We shall say that an FMRA is of *inexact/exact type* if $\{\tau_k\phi : k \in \mathbf{Z}\}$ is an inexact/exact frame for the subspace V_0. For detail analysis and constructions of FMRAs, see [1], [3]. *The frame multiresolution subspaces* are the subspaces $V_j \equiv \overline{sp}\{\phi_{jk}\}_k$ defined in an FMRA, where $\phi_{jk} \equiv \sqrt{2^j}\phi(2^j t - k)$.

The redundancy inherent in frame decompositions can be used for noise reduction, e.g., [4], where a finite dimensional example exhibits the procedure. We can generalize the example is the following way:

Proposition 2.2 *Let $\{x_n\}$ be a tight frame for $\mathcal{H}$, a separable Hilbert space, with frame bounds $A = B > 1$ and each $\|x_n\| = 1$. Let $\{e_n\}$ be an orthonormal basis (ONB) of $\mathcal{H}$, and let $\{w_n\}$ be a sequence of independent identical random variables with 0 mean and such that $\sum Var(w_n) = 1$. Consider the representation of a signal in $\mathcal{H}$ in terms of the ONB and the frame, i.e.,*

$$\forall f \in \mathcal{H}, \quad f = \sum \langle f, e_n \rangle e_n,$$

and

$$\forall f \in \mathcal{H}, \quad f = \frac{1}{A}\sum \langle f, x_n \rangle x_n,$$

respectively. If the coefficients $\{\langle f, e_n\rangle\}$ and $\{\langle f, x_n\rangle\}$ are both perturbed component-wise by random noise $\{\epsilon w_n\}$, then the expected reconstruction error due to the noise is less in the frame expansion than in the ONB expansion. In fact, there is a gain of $(1 - \frac{1}{A^2})$ in the frame case over the ONB case.

Proof: The expected error for the ONB case is defined as

$$\begin{aligned} \mathbf{E}\|f - \sum(\langle f, e_n\rangle + \epsilon w_n)e_n\|^2 &= \mathbf{E}\|\sum \epsilon w_n e_n\|^2 \\ &= \epsilon^2 \mathbf{E}\|\sum w_n e_n\|^2 \\ &= \epsilon^2 \int_P (\int_R |\sum w_n(\alpha)e_n(t)|^2 dt) d\mu(\alpha) \\ &= \epsilon^2 \int_P \sum |w_n(\alpha)|^2 d\mu(\alpha) = \epsilon^2, \end{aligned}$$

where $\mathbf{E}$ designates expectation, μ is the probability measure, and P is the probability space.

In the case of tight frame $\{x_n\}$ with frame bounds $A = B > 1$, the expected error is

$$\begin{aligned}
& \mathbf{E}\|f - \frac{1}{A}\sum(\langle f, x_n\rangle + \epsilon w_n)x_n\|^2 \\
= & \mathbf{E}\|\frac{1}{A}\sum \epsilon w_n x_n\|^2 \\
= & \frac{\epsilon^2}{A^2}\mathbf{E}\|\sum w_n e_n\|^2 \\
= & \frac{\epsilon^2}{A^2}\int_P(\int_R|\sum w_n(\alpha)e_n(t)|^2 dt)d\mu(\alpha) \\
= & \frac{\epsilon^2}{A^2}\int_P(\sum|w_n(\alpha)|^2\int_R|x_n(t)|^2 dt + \int_R\sum_{m\neq n} w_m(\alpha)\bar{w_n}(\alpha)x_m(t)\bar{x_n}(t)dt)d\mu(\alpha) \\
= & \frac{\epsilon^2}{A^2}\sum_{m\neq n}\int_R x_m(t)x_n(t)dt\int_P w_m(\alpha)\bar{w_n}(\alpha)d\mu(\alpha) + \frac{\epsilon^2}{A^2}\int_P\sum|w_n(\alpha)|^2 d\mu(\alpha) \\
= & \frac{\epsilon^2}{A^2}.
\end{aligned}$$

We see that there is a gain of $1 - \frac{1}{A^2}$ over the ON system.

This establishes the result. ■

The construction of tight frames with $A = B > 1$ can be made using the following result [3].

Proposition 2.3 *Let $\phi \in L^2(\mathbf{R})$. Assume $supp(\hat{\phi})$ is an interval in $[-\frac{1}{2}, \frac{1}{2})$. Then $\{\tau_n\phi\}$ is a tight inexact frame for $V_0 \equiv \overline{sp}\{\tau_n\phi\}$ with frame bounds $A = B$ if and only if*

$$\Phi(\gamma) = A, \quad a.e.\ on\ [0,1)\setminus\mathbf{N}, \tag{1}$$

where $\Phi(\gamma) \equiv \sum_k|\hat{\phi}(\gamma + k)|^2$, $\mathbf{N} \equiv \{\gamma \in [0,1) : \Phi(\gamma) = 0\}$ and $|\mathbf{N}| > 0$. In particular, if $\|\phi\|_2 = 1$, then the frame bound $A > 1$.

Proof: We proved in [1], [3] that $\{\tau_n\phi\}$ forms a frame for $V_0 \equiv \overline{sp}\{\tau_n\phi\}$ with frame bounds A and B if and only if

$$A \leq \Phi(\gamma) \leq B \quad a.e.\ on\ [0,1)\setminus\mathbf{N}.$$

Therefore, because of (1), $\{\tau_n\phi\}$ is a tight frame for $V_0 \equiv \overline{sp}\{\tau_n\phi\}$ with frame bounds A.

Now, assume $\|\phi\|^2 = 1$. Since supp $\hat{\phi}$ is an interval in $[-\frac{1}{2}, \frac{1}{2})$, $\Phi = \hat{\phi}$ in $[-\frac{1}{2}, \frac{1}{2})$. Hence,

$$1 = \|\phi\|^2 = \|\hat{\phi}\|^2 = \int_{N^c} A^2 = A^2|\mathbf{N}^c|,$$

where $\mathbf{N}^c \equiv [0,1)\setminus\mathbf{N}$. Since $|\mathbf{N}| > 0$, we have $|\mathbf{N}^c| < 1$. Consequently, $A > 1$. ■

Thus, by *Proposition 2.2*, the representation of signals in a frame multiresolution subspace V_j generated by such a frame is less sensitive to noise of the above form than when dealing with an ONB.

By the theory of FMRAs, for any signal $f \in L^2(\mathbf{R})$ and arbitrary $\epsilon > 0$, there exists a J and a function $g \in V_J$ such that

$$\|f - g\|_2 < \epsilon,$$

and the best approximation of f in V_J for tight frames is

$$\tilde{f} = \frac{1}{A} \sum_k \langle f, \phi_{Jk} \rangle \phi_{Jk}. \tag{2}$$

Assume that the procedure of finding the appropriate scale J and the sampling/representation of f in terms of (2) belongs to the pre-filtering [2], [3]. Without loss of generality, we shall concentrate on the basic frame multiresolution subspace V_0 due to the similarity of each V_j in FMRAs. Then the subband processing consists of the usual decomposition and reconstruction steps, viz.,

(a) Decomposition

$$c_{-1}(n) \equiv \langle f, \phi_{-1,n} \rangle = \sum_k \overline{h_0(k-2n)} c_0(k),$$

$$d_{-1}(n) \equiv \langle f, \phi_{-1,n} \rangle = \sum_k \overline{g_0(k-2n)} c_0(k),$$

and

(b) Reconstruction

$$c_0(n) = \sum_k \overline{h_1(2k-n)} c_{-1}(k) + \sum_k \overline{g_1(2k-n)} d_{-1}(k),$$

where $c_0 = \langle f, \phi_{0k} \rangle$.

A complete subband system in the frame multiresolution subspace V_0 can then be summarized by the following figure,

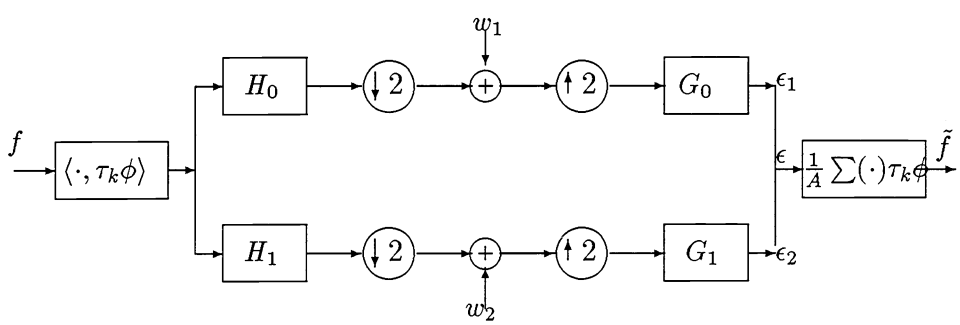

Figure 1. A subband signal processing system in frame multiresolution subspaces

where H_0, H_1 and G_0, G_1 are the analysis and synthesis filters associated with a given FMRA [3], ϵ_1, ϵ_2 are output noise of upper and lower channels corresponding to quantization noise inputs w_1, w_2, respectively, and $\epsilon(n) \equiv \epsilon_1(n) + \epsilon_2(n)$. These notions are described in *Section 3.*

3 The Quantization Noise Model and Noise Propagation in a Subband System

Since one of the fundamental purposes of subband processing is to achieve greater data compression, quantization at subbands is a key element in subband coding systems. Therefore, the effect and noise introduced by quantization and its consequences at the output of the whole system is an extremely important issue. There is a large literature dealing with the subject, where the quantization effect is integrated into the subband filtering system to optimize the design of the filter bank, e.g., [5], [9], [11], [13].

One of our purposes in this paper is to look at this issue from a new point of view. While almost all existing subband filter banks correspond to some type of orthogonal or biorthonormal basis in terms of wavelet theory, we shall demonstrate that significant noise reduction is achieved by simply using wavelet frames and their associated filter banks. The structure of FMRAs and the redundancy they model provide a natural tool for noise suppression.

Understanding the behavior of quantization noise and its propagation in a subband system is essential for reducing it, and the quantization model has been studied in the past, e.g., [6]. It is known that, for the pdf-optimized quantizer [5], [6], the quantization error can be modeled by an unbiased additive noise, and that the error is uncorrelated to the quantizer output. Such a quantization model is not generally input signal independent. However, with a gain-plus-additive noise model, the quantization effect is very well represented [6]. Therefore, without loss of generality, we shall adopt such a model in our study of the quantization noise effect. We shall also assume that the gain in the quantization model is 1. Hence, the quantization noise will be modeled by an additive white noise process as shown in Figure 1.

The next important issue is about the propagation of the quantization noise in the synthesis operations. The decimation and interpolation in a subband system are time-varying linear devices which affect the behavior of noise propagation. It is shown [8], [10] that if a filter is such that the decimation of its impulse response does not create aliasing, the output of each synthesis channel (with interpolation and filtering) will be a wide sense stationary process (WSS) for given WSS inputs. In particular, when the synthesis filters G_0 and G_1 are ideal filters, the outputs are band-limited white noise for white noise inputs.

Adopting the usual quantization noise modeling and basic assumptions and results outlined above, we can verify the following proposition about noise reduction.

Proposition 3.1 *Let $\{\phi(t-k)\}$ be a tight inexact frame for the frame subspace V_0 associated with an FMRA. Let $\|\phi\|_2 = 1$, so that the frame constant $A > 1$. Assume that the additive noise processes w_1 and w_2 are 0-mean uncorrelated white processes with variances σ_1^2 and σ_2^2, respectively. Then there exist synthesis filters G_0 and G_1 associated with the FMRA such that the expectation of the reconstruction error is*

$$\mathbf{E}\|f-\tilde{f}\|^2 = \frac{1}{A^2}(\eta\sigma_1^2 + \eta\sigma_2^2 + \mathbf{E}(\sum_{k\neq n}\epsilon(k)\epsilon(n)\langle\phi, \tau_{n-k}\phi\rangle)),$$

where $\eta < \frac{1}{2}$ is the bandwidth of G_0 and G_1.

Proof: With the quantities defined in Figure 1, we have the following computation.

$$\begin{aligned}
\mathbf{E}\|f-\tilde{f}\|^2 &= \mathbf{E}\|\frac{1}{A}\sum_k(\epsilon_1(k)+\epsilon_2(k))\phi(t-k)\|^2 \\
&= \frac{1}{A^2}\mathbf{E}\|\sum_k \epsilon(k)\phi(t-k)\|^2 \\
&= \frac{1}{A^2}\mathbf{E}\sum_k\sum_n \epsilon(k)\bar{\epsilon}(n)\langle\phi, \tau_{n-k}\phi\rangle \\
&= \frac{1}{A^2}\mathbf{E}\sum_k |\epsilon(k)|^2 + \sum_{k\neq n}\epsilon(k)\bar{\epsilon}(n)\langle\phi, \tau_{n-k}\phi\rangle
\end{aligned}$$

$$= \frac{1}{A^2}(\mathbf{E}(\sum_k |\epsilon_1(k)|^2 + \sum_k |\epsilon_1(k)|^2 + 2Re(\sum_k \epsilon_1(k)\bar{\epsilon_2}(k)))) +$$
$$\frac{1}{A^2}\mathbf{E}(\sum_{k\neq n} \epsilon(k)\bar{\epsilon}(n)\langle\phi, \tau_{n-k}\phi\rangle)$$
$$= \frac{1}{A^2}(\mathbf{E}(\sum_k |\epsilon_1(k)|^2) + \mathbf{E}(\sum_k |\epsilon_1(k)|^2) + \mathbf{E}(\sum_{k\neq n} \epsilon(k)\bar{\epsilon}(n)\langle\phi, \tau_{n-k}\phi\rangle)).$$

It is known [8] that the power spectral density of ϵ_1 and ϵ_2 are $\sigma_1^2|G_0|^2$ and $\sigma_2^2|G_1|^2$, respectively. Therefore,

$$\mathbf{E}||f - \tilde{f}||^2 = \frac{1}{A^2}(\eta\sigma_1^2 + \eta\sigma_2^2 + \mathbf{E}(\sum_{k\neq n} \epsilon(k)\epsilon(n)\langle\phi, \tau_{n-k}\phi\rangle)),$$

where η is the bandwidth of G_0 and G_1. By the inexact frame hypothesis, $\eta < \frac{1}{2}$. ■

Remark 3.2 If a subband system as in Figure 1 is built in a subspace generated by an ONB in terms of ideal filters, it is standard to see that the expected reconstruction error is

$$\mathbf{E}||f - \tilde{f}||^2 = (\tfrac{1}{2}\sigma_1^2 + \tfrac{1}{2}\sigma_2^2);$$

in fact,

$$\begin{aligned}
\mathbf{E}||f - \tilde{f}||^2 &= \mathbf{E}||\sum_k(\epsilon_1(k) + \epsilon_2(k))\phi(t-k)||^2 \\
&= \mathbf{E}(\sum_k\sum_n(\epsilon_1(k) + \epsilon_2(k))\overline{(\epsilon_1(k) + \epsilon_2(k))}\langle\tau_k\phi, \tau_n\phi\rangle) \\
&= \mathbf{E}(\sum_k ||\epsilon_1(k)||^2 + \sum_k ||\epsilon_2(k)||^2 + 2Re(\sum_k \epsilon_1(k)\bar{\epsilon_2}(k)) \\
&= \mathbf{E}(\sum_k ||\epsilon_1(k)||^2) + \mathbf{E}(\sum_k ||\epsilon_2(k)||^2) \\
&= \tfrac{1}{2}(\sigma_1^2 + \sigma_2^2),
\end{aligned}$$

where we have used the fact the synthesis filters in the position of G_0 and G_1 in Figure 1 have bandwidth $\frac{1}{2}$.

4 Numerical Examples

Example 4.1 Let $\hat{\phi}(\gamma) = c\mathbf{1}_{[-\frac{1}{4},\frac{1}{4}]}(\gamma)$. It can be shown that $\{\tau_n\phi\}$ forms a tight inexact frame for $V_0 \equiv \overline{sp}\{\tau_n\phi\}$ with frame bounds $A = B = |c|^2$, and ϕ generates an FMRA [3]. To obtain $||\phi||_2 = 1$, we need $A = |c|^2 = 2 > 1$.

If $\{h_0(n)\}$ is the analyzing filter defining the scaling equation, then

$$\phi(t) = \sqrt{2}\sum_n h_0(n)\phi(2t-n)$$

or

$$\hat{\phi}(\gamma) = \frac{1}{\sqrt{2}}H_0(\frac{\gamma}{2})\hat{\phi}(\frac{\gamma}{2}), \tag{3}$$

where $H_0(\gamma) \equiv \sum h_0(n) e^{-2\pi i n\gamma}$.

Now that $\hat{\phi}$ is given, we can determine H_0 from equation (3). Note that, due to the nonuniqueness of the frame representation, the choice of H_0 is not unique. We may take, e.g.,

$$H_0(\gamma) = \sqrt{2}\mathbf{1}_{[-\frac{1}{8},\frac{1}{8})}(\gamma).$$

It can also be shown [1] that the band-pass analyzing filter may be chosen as

$$H_1(\gamma) = \sqrt{2}\mathbf{1}_{[-\frac{1}{4},-\frac{1}{8})}(\gamma) + \sqrt{2}\mathbf{1}_{[\frac{1}{8},\frac{1}{4})}(\gamma),$$

and we can take the synthesizing filters G_0 and G_1 such that

$$|G_0(\gamma)| = |H_0(\gamma)| \quad \text{a.e.},$$

and

$$|G_1(\gamma)| = |H_1(\gamma)| \quad \text{a.e.}.$$

The filters H_0, H_1, G_0, G_1 form a perfect reconstruction filter bank associated with an FMRA. We have therefore constructed a subband system in a frame multiresolution subspace.

Figures 2 to 9 are numerical results to compare the noise reduction performances of MRA, e.g., [7], [12], and FMRA processing. In all figures, the top picture is the original signal. For the identical noise and noise power introduced in the quantization process, the middle and the bottom pictures are the results using the Haar quadrature mirror filters (QMF) and the associated filters of an FMRA in the above example, respectively. In figures 1 to 4, an actual scan line of an MRI image is used in simulation. In figures 5 to 8, a chirp signal is studied.

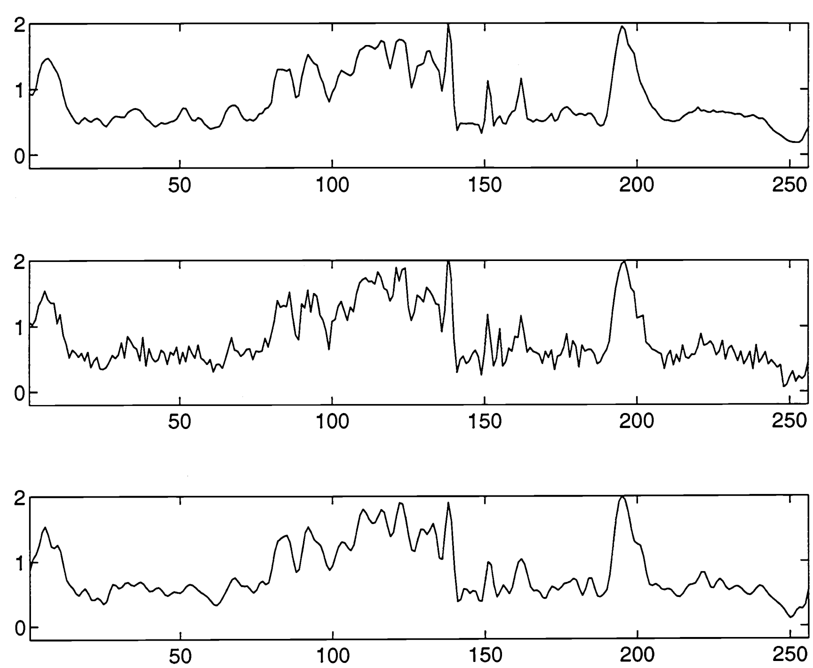

Figure 2. The top picture is the original signal, a scan line of an MRI image. The middle picture is the result when the Haar QMF is used. The bottom picture is the result when the FMRA filters in example 4.1 are used. The noise introduced at the quantization stage is a white Gaussian noise having mean 0 and variance 0.01.

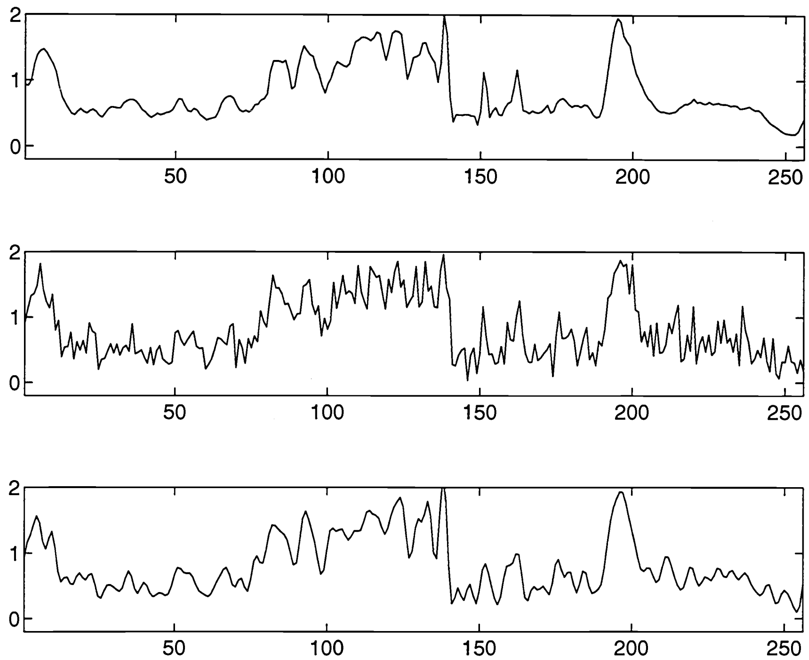

Figure 3. The top picture is the original signal, a scan line of an MRI image. The middle picture is the result when the Haar QMF is used. The bottom picture is the result when the FMRA filters in example 4.1 are used. The noise introduced at the quantization stage is a white Gaussian noise having mean 0 and variance 0.04.

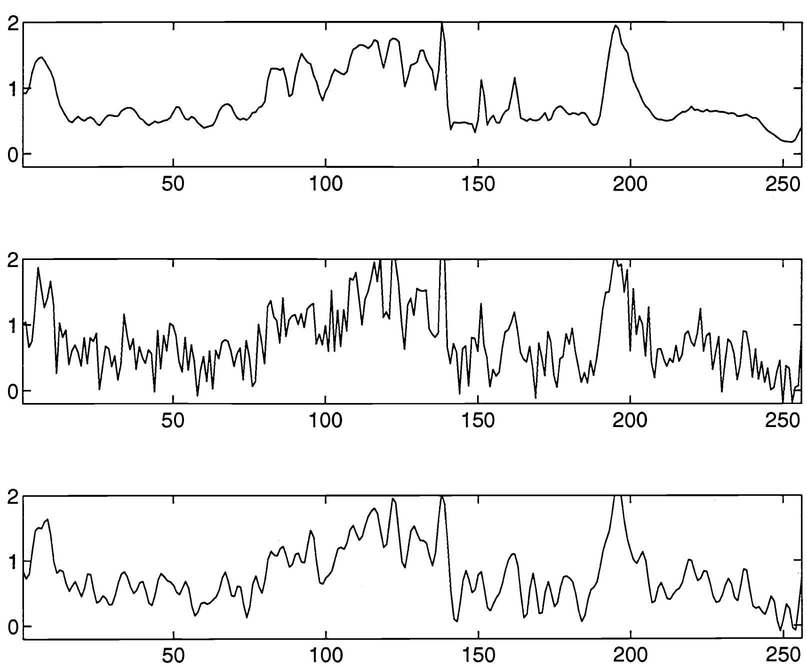

Figure 4. The top picture is the original signal, a scan line of an MRI image. The middle picture is the result when the Haar QMF is used. The bottom picture is the result when the FMRA filters in example 4.1 are used. The noise introduced at the quantization stage is a white Gaussian noise having mean 0 and variance 0.09.

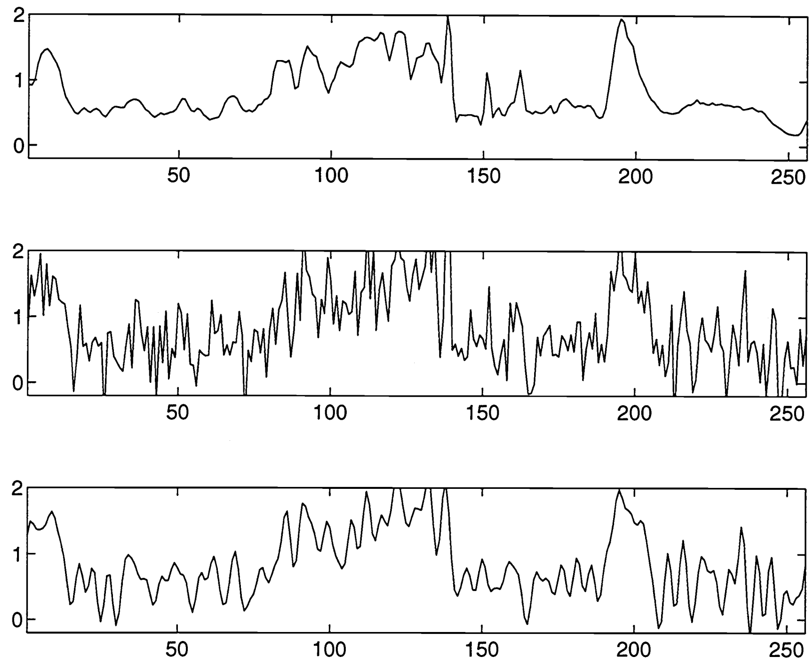

Figure 5. The top picture is the original signal, a scan line of an MRI image. The middle picture is the result when the Haar QMF is used. The bottom picture is the result when the FMRA filters in example 4.1 are used. The noise introduced at the quantization stage is a white Gaussian noise having mean 0 and variance 0.16.

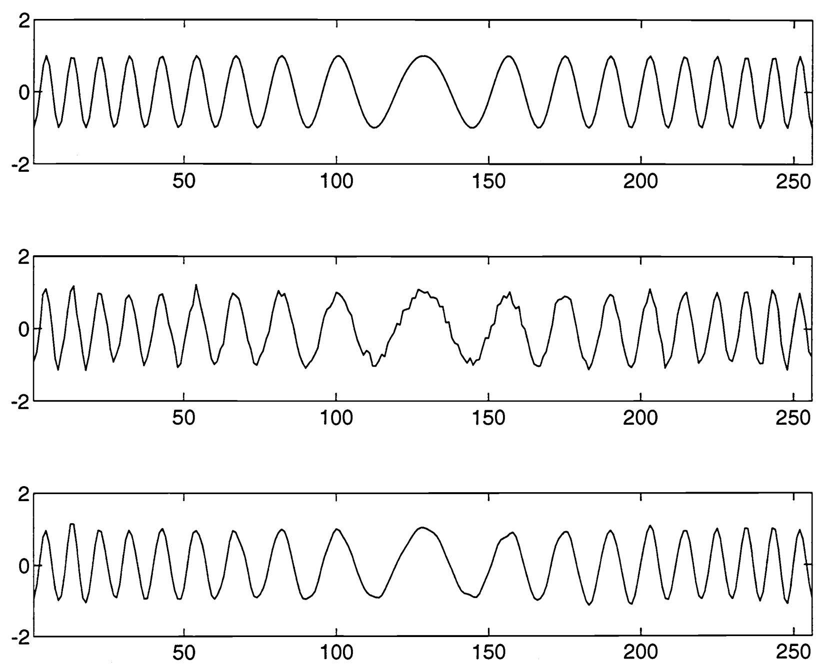

Figure 6. The top picture is the original signal, a chirp signal. The middle picture is the result when the Haar QMF is used. The bottom picture is the result when the FMRA filters in example 4.1 are used. The noise introduced at the quantization stage is a white Gaussian noise having mean 0 and variance 0.01.

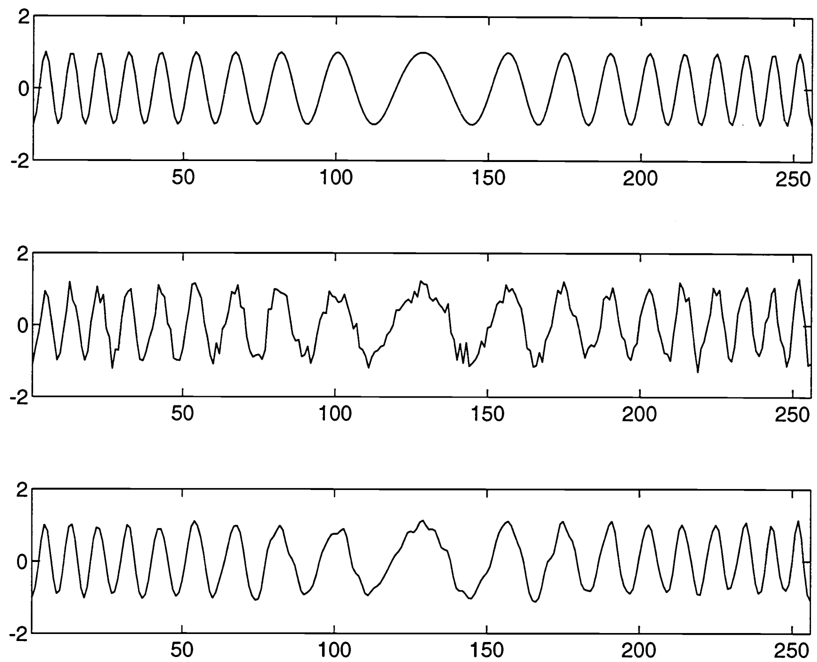

Figure 7. The top picture is the original signal, a chirp signal. The middle picture is the result when the Haar QMF is used. The bottom picture is the result when the FMRA filters in example 4.1 are used. The noise introduced at the quantization stage is a white Gaussian noise having mean 0 and variance 0.04.

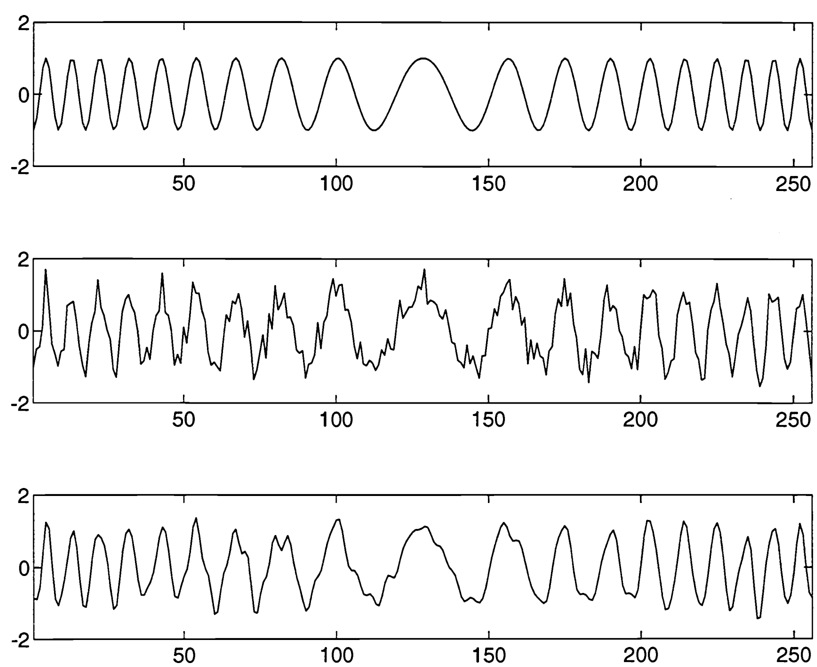

Figure 8. The top picture is the original signal, a chirp signal. The middle picture is the result when the Haar QMF is used. The bottom picture is the result when the FMRA filters in example 4.1 are used. The noise introduced at the quantization stage is a white Gaussian noise having mean 0 and variance 0.09.

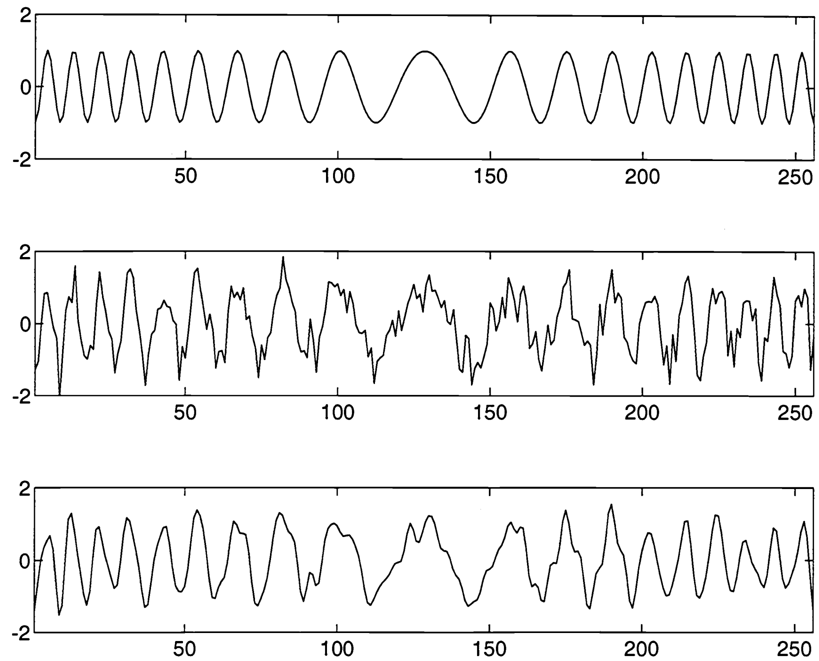

Figure 9. The top picture is the original signal, a chirp signal. The middle picture is the result when the Haar QMF is used. The bottom picture is the result when the FMRA filters in example 4.1 are used. The noise introduced at the quantization stage is a white Gaussian noise having mean 0 and variance 0.16.

References

[1] J. J. Benedetto and S. Li. Multiresolution analysis frames with applications. *ICASSP'93, Minneapolis, April 26-30*, III: pp304–307, 1993.

[2] J. J. Benedetto and S. Li. Narrow band frame multiresolution analysis with perfect reconstruction. submitted to IEEE-SP Symposium on TF-TS, October, 1994.

[3] J. J. Benedetto and S. Li. The theory of multiresolution analysis frames and applications to filter banks. *preprint*, 1994.

[4] I. Daubechies. *Ten Lectures on Wavelets.* SIAM, Philadelphia, 1992.

[5] R. A. Haddad, K. Park, and N. Uzun. Optimum (MSE) design of quantized M-band filter banks. *preprint*, 1994.

[6] N. S. Jayant and P. Noll. *Digital Coding of Waveforms.* Prentice Hall, 1984.

[7] S. Mallat. A theory of multiresolution signal decomposition: The wavelet representation. *IEEE PAMI*, 11, No. 7: pp674–693, 1989.

[8] V. P. Sathe and P. P. Vaidyanathan. Effects of multirate systems on the statistical properties of random signals. *IEEE Trans. Signal Processing*, 41, No. 1: pp131–146, 1993.

[9] A. Tabatabai. Optimum analysis/synthesis filter bank structures with application to subband coding systems. *Proc. IEEE ICASSP'88*, pages pp823–826, 1988.

[10] P.P. Vaidyanathan. Multirate digital filters. *IEEE Proceedings*, 78, 1990.

[11] L. Vandendorpe. Optimized quantization for image subband coding. *Signal Processing, Image Communication,* Elsevier, Amsterdam, Nov., 4, No.1: pp65–80, 1991.

[12] M. Vetterli and C. Herley. Wavelets and filter banks: theory and design. *IEEE ASSP*, 40, No. 9: pp2207–2232, 1992.

[13] P. H Westerink, J. Biemond, and D. E. Boekee. Scalar quantization error analysis for image subband coding using qmf's. *IEEE Trans. Signal Processing*, 40, No. 2: pp421–428, 1992.